

# Data Augmentation of Spectral Data for Convolutional Neural Network (CNN) Based Deep Chemometrics

Esben Jannik Bjerrum<sup>1,\*</sup>, Mads Glahder<sup>1</sup> and Thomas Skov<sup>2</sup>

<sup>1</sup> Wildcard Pharmaceutical Consulting, Zeaborg Science Center, Frødings Allé 41, 2860 Søborg, Denmark.

<sup>2</sup> Spectroscopy and Chemometrics, Department of Food Science, Copenhagen University, Rolighedsvej 26, 1958 Frederiksberg, Denmark

\* Corresponding Author: esben@wildcardconsulting.dk

Deep learning methods are used on spectroscopic data to predict drug content in tablets from near infrared (NIR) spectra. Using convolutional neural networks (CNNs), features are extracted from the spectroscopic data. Extended multiplicative scatter correction (EMSC) and a novel spectral data augmentation method are benchmarked as preprocessing steps. The learned models perform better or on par with hypothetical optimal partial least squares (PLS) models for all combinations of preprocessing. Data augmentation with subsequent EMSC in combination gave the best results. The deep learning model CNNs also outperform the PLS models in an extrapolation challenge created using data from a second instrument and from an analyte concentration not covered by the training data. Qualitative investigations of the CNNs kernel activations show their resemblance to wellknown data processing methods such as smoothing, slope/derivative, thresholds and spectral region selection.

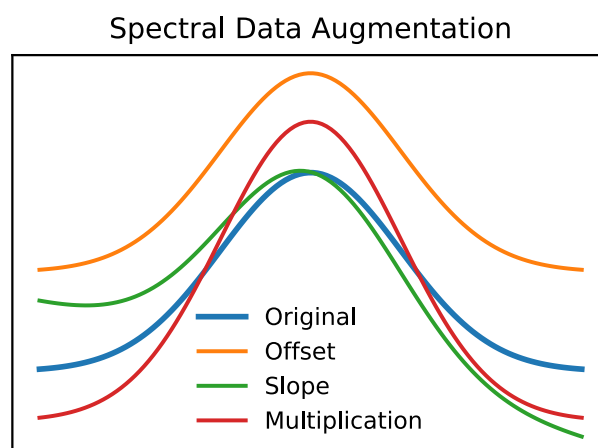
## Introduction

Use of artificial neural networks (ANNs) for analysis of spectroscopic data is decades old[1] and they have been widely used as nonlinear models for the analysis of spectroscopic data. Convolutional neural networks (CNNs)[2, 3] are ANNs with a special layout and restrictions that make them excellent for modelling spatial data. Neighboring data points are analysed in mini networks by “scanning” the data with a limited spatial width (filter size). This is done multiple times with different mini networks (kernels). The trained weights for the mini network for each kernel must be the same for the entire sweep of the data. In image analysis and classification these ANN types surpassed human interpretation two years ago[4]. The activations of the kernels are then fed forward in the neural network into new convolutional layers or standard dense layers.

A spectrum can be thought of as a one-dimensional picture, and this type of neural network architecture has recently been used for spectroscopical data. As examples they were employed for classification of Raman Spectra[5] and for classification of pharmaceutical tablets using VIS-NIR spectroscopy[6]. CNNs have also been used for regression modelling of NIR and Raman Data, including advanced spectral region selection via a custom regularization function.[7]

Data augmentation is a wellknown technique for improving robustness and training of neural networks[2]. It has been used with success in many domains ranging from image classification[8] to molecular modelling[9]. The core idea is to expand the number of training samples from the limited number of labelled samples by simulating various expected

**Figure 1:** Components of the spectral data augmentation. Data augmentation is created with randomly scaled contributions from offset, slope and multiplication to simulate baseline offset, slope differences and differences in intensity in the spectral recordings.



variations in the datasets. For images it is easy to understand that a picture of a cat is recognisable even though it has been rotated randomly between  $-45^\circ$  to  $45^\circ$  or flipped. The neural network subsequently learns how to cope with such variations resulting in a more robust training. For spectral data the variation employed is suggested as in Figure 1. Here random offsets, random changes in slope and random multiplications are added to the existing spectrums to expand the dataset.

Dropout[10] is a wellknown regularization technique employed for deep learning neural network models. During training each activation (or data input

---

point) is randomly dropped/removed from the vector fed into the subsequent layer with a tunable probability (the dropout rate). The effect is a disruption of the neuron interdependence, so that each neuron can't make predictions on very specific patterns of the input. This in turn leads to more independent neurons and redundancy in the data handling. This limits the overfitting capacity and give better generalization for prediction of novel samples. After training the weights of the layer are scaled proportionally to the dropout rate and the dropout layer is not active during sampling.

Here we analyze a tablet dataset[11, 12] using CNNs with automatic tuning of the model hyperparameters and regularization level in the form of dropout layers. The dataset consists of assay results from analysis of pharmaceutical tablets and NIR spectra recorded with two different instruments. Data preprocessing in the form of spectral data augmentation is implemented and the performance compared with extended multiplicative scatter correction (EMSC). All dataset treatments are compared to hypothetical optimal PLS models as a baseline method. The model types performances are also compared on a specially crafted extrapolation challenge for both assay result values and instrument recordings.

## Methods

### Datasets

The dataset was downloaded[12] and read from Matlab format into Python using utilities from Scientific Python[13]. The original data from instrument one and two was pooled on their own, and divided into different training, validation and external test sets. A standard dataset split was created by randomly splitting off 20% for test and validation set in successive steps. The extrapolation set was split into sets with the test set having measured concentration above 228mg, the validation set between 228mg and 212mg and the training set with concentrations below 212mg. The training and validation sets was exclusively done with spectrums obtained with instrument one, whereas the test sets were exclusively taken from instrument two. The spectral region from 600 to 1798 nm was used for modelling.

**Outlier removal** Spectral outliers were identified by PLS modeling, using the implementation of the NIPALS algorithm[14] in Scikit-Learn[15], without scaling and a maximum of 100.000 iterations and a tolerance of  $10^{-16}$ . The entire dataset was subjected to 10 fold cross validation (CV) varying the number of principal components between 1 and 30. The number of principal components that gave the lowest average Huber loss[16] for the cross validation sets was used to model the entire dataset and the outliers identified as

samples having more than 2.5 times the standard deviation of the absolute error of prediction.

**Data Augmentation** Some of the datasets were augmented by adding random variations in offset, multiplication and slope. Offset was varied  $\pm 0.10$  times the standard deviation of the training set. Multiplication was done with  $1 \pm 0.10$  times the standard deviation of the training set, and the slope was adjusted uniformly randomly between 0.95 to 1.05. This was done 9 times for each sample in the training set and appended to the dataset. The assay reference set was expanded appropriately.

### Extended Multiplicative Scatter Correction

Some of the datasets were subjected to Extended Multiplicative Scatter Correction (EMSC)[17] with an order of one. The EMSC python code was adapted from the ChemPy project[18]. The reference spectrum was the average of the training set for EMSC correction of all the dataset subsets.

**Normalization** All datasets were normalized by subtracting the global mean of the training set and dividing by two times the global standard deviation of the training ensuring that most of the values are in the range -1 to 1.

### Neural Networks

A CNN was built by using Keras v.1.2.2[19] with Theano v.0.9.0[20] as the computation back end. GPU computation was done using CUDA version 8.0.[21] The input was fed to a Gaussian noise layer with a standard deviation of 0.01, followed by two one-dimensional convolutional layers[22, 23] with a rectified linear activation.[24] The output from the convolutional kernels were flattened and a dropout layer[10] was added before connecting to a fully connected dense layer with a linear activation function. The output layer was a single dense neuron with a linear activation function. The loss function was a Huber loss[16] adapted for use with Keras. Training was done with the Adadelta optimizer[25].

### Hyperparameter tuning and training

The hyperparameters for the neural network listed in Table 1 was optimized using Bayesian optimization with Gaussian processes as implemented in the Python package GpyOpt[26] version 1.0.3. The optimization was initialized with 20 random parameter sets followed by up to 40 iterations of standard Gaussian process optimization with the expected improvement acquisition function. In each iteration a new network was built from the parameter set and trained for 40 or 200 epochs, with learning rates of 0.084 and 0.094 for

**Table 1:** hyperparameter search space, l1: Layer 1, l2: Layer 2, Conv: Convolutional

Parameter	Search Space	Type
Conv l1 no. Kernels	2 - 40	Integer
Conv l1 Filter size	5 - 150	Integer
Conv l2 no. Kernels	2 - 40	Integer
Conv l2 Filter size	5 - 150	Integer
Dropout after Flatten	0 - 0.5	Float
Dense no. Neurons	4 - 1000	Integer

datasets with and without data augmentation, respectively. Batch size was set to 45. The loss function was taken as an average of the validation loss observed for the last 10 epochs of training.

Final training of the neural networks was done with the identified optimized architecture and hyperparameters for each dataset and preprocessing type. The training was extended to 100 and 250 epochs for datasets with and without data augmentation, respectively. The learning rate was reduced with a factor of two when the validation loss failed to improve for 10 or 25 epochs (DA/non-DA).

The number of components for the PLS model was tuned by identifying the number of components that gave the lowest Huber loss on the test set when trained on the pooled validation and training sets. Additionally CV loss and training loss were recorded and used to calculate a corrected CV loss, where the difference between the training loss and the CV loss is added to the CV loss.

All computations and training were done on a Linux workstation (Ubuntu Mate 16.04 LTS) with 32GB of RAM, i5-2405S CPU @ 2.50GHz and an Nvidia Geforce GTX1060 graphics card with 6 GB of RAM.

## Results

The two different ways of splitting into subsets and the different selected preprocessing steps resulted in the datasets listed in Table 2. The employed data augmentation resulted in a 10 fold increase in training and validation set size, whereas the test set was not data augmented. Splitting for the extrapolation datasets based on assay values resulted in validation and test set sizes of 52 and 13, respectively. Each datasets hyperparameters were optimized on its own, by optimizing the predictive performance on the validation set for the CNN models. An example of the convergence of the optimization is shown in Figure 2. After the first 20 randomly selected parameter sets, the optimization algorithm chooses the next parameter set to test, finding the best solution at iteration 41.

In contrast to the use of validation sets for tuning the CNNs, the hyperparameters of the PLS models were optimised with respect to the test set. An example of the tuning curve for the Standard set is shown in Fig-

**Figure 2:** Example convergence of the hyperparameter tuning (EMSC dataset). The blue line shows the loss for the validation set at a given iteration. The first 20 iterations are randomly selected hyperparameters and the rest are hyperparameters chosen by the bayesian optimizer from GPyOpt. The dashed grey line shows the loss of the best found hyperparameter set at a given iteration. The best solution was found at iteration 41.

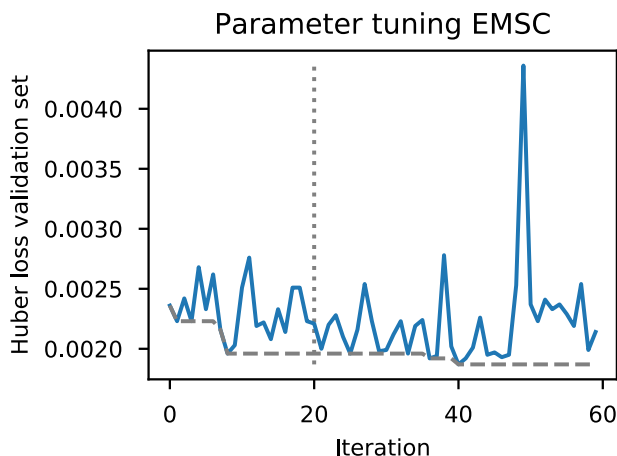
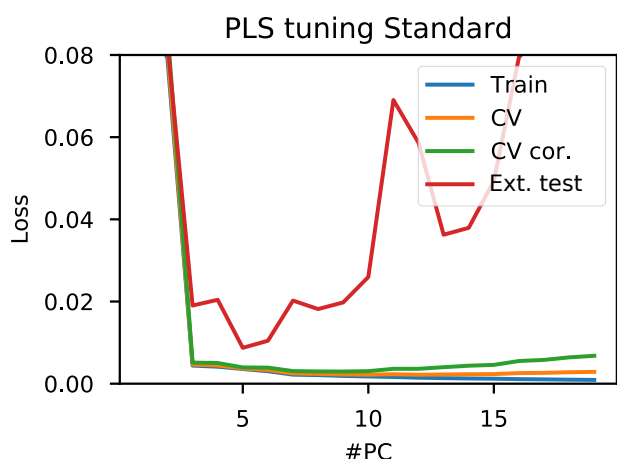


**Figure 3:** Example of the PLS hyperparameter tuning. The performance using the Huber loss is followed as the number of principal components is varied.



ure 3. The red curve has the lowest loss at five components, whereas the CV and Corrected CV have minimums at 10 and 9 components, respectively. Using the minimum of the corrected validation loss or validation loss directly in general resulted in larger number of PLS components to be included and lower predictive performance for the test set.

The found hyperparameters are listed in Table 3 and 4 for the datasets without and with data augmentation, respectively. The dropout rate is in the low range for most of the datasets. The number of kernels for layer two seem on average to be larger or the same as layer one with the DA EMSC dataset as an exception. Figure 4 shows a comparison between the training histories for the EMSC dataset with and without data augmentation. Both training histories in the end obtain a low difference between the training and val-

**Table 2:** Details of the datasets used. GS: Global scaling, DA: Data Augmentation, EMSC: Extended multiplicative scatter correction

Dataset	Preprocessing	Size		
		Training	Validation	Test
Standard	GS	404	101	136
EMSC	EMSC + GS	404	101	136
Extrapolation (Ext.)	GS	576	52	13
Ext. EMSC	EMSC + GS	576	52	13
Data Augmentation (DA.)	DA + GS	4040	1010	136
DA EMSC	DA + EMSC + GS	4040	1010	136
Ext. DA	DA + GS	5760	520	13
Ext. DA EMSC	DA + EMSC + GS	5760	520	13

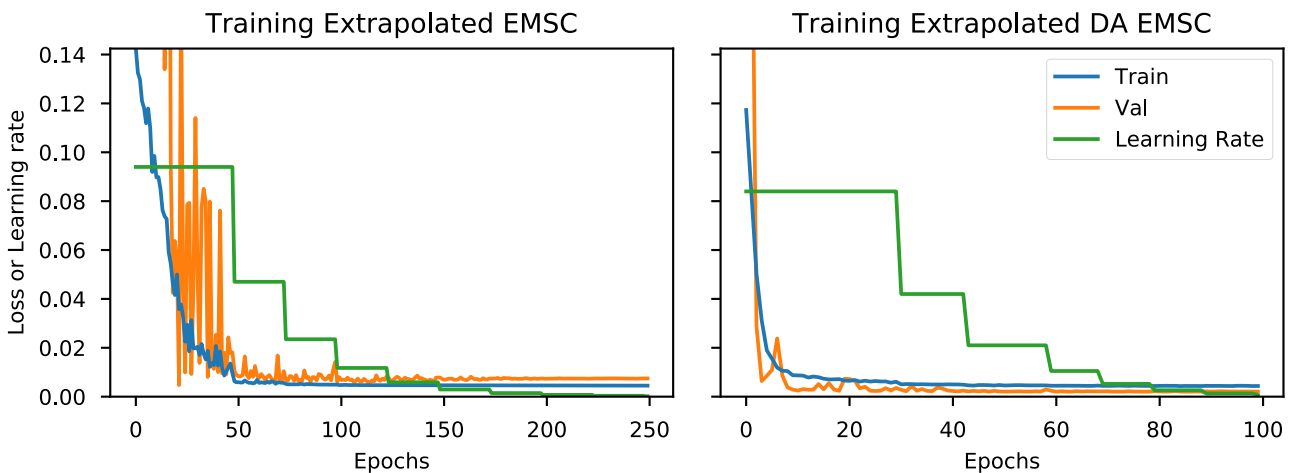
**Table 3:** Optimized hyperparameters for datasets without data augmentation. Ext: Extrapolation, EMSC: Extended multiplicative scatter correction

Parameter	Standard	EMSC	Ext.	Ext. EMSC
Conv layer 1 no. Kernels	14	18	22	40
Conv layer 1 Filter size	29	40	45	96
Conv layer 2 no. Kernels	30	18	25	40
Conv layer 2 Filter size	22	29	40	45
Dropout after Flatten	0.045	0.070	0.082	0.0
Dense Layer no. Neurons	176	266	468	470
Principal Components	5	4	8	6

**Table 4:** Optimized hyperparameters for datasets with data augmentation. Ext: Extrapolation, EMSC: Extended multiplicative scatter correction.

Parameter	DA	DA EMSC	Ext. DA	Ext. DA EMSC
Conv layer 1 no. Kernels	29	19	7	22
Conv layer 1 Filter size	124	138	80	54
Conv layer 2 no. Kernels	28	5	24	29
Conv layer 2 Filter size	119	54	60	42
Dropout after Flatten	0.205	0.089	0.015	0.388
Dense Layer no. Neurons	289	527	749	289
Principal Components	5	4	9	7

**Figure 4:** Example training history comparing a dataset with and without data augmentation.



---

validation loss for many epochs in the end of training, indicating absence of overfitting. The validation loss displays a much rougher curve over the course of training for the dataset without data augmentation.

The measured model performance for the different dataset splits and preprocessing selections is shown in Table 5. The neural network models show better performance for most of the datasets with respect to the RMSE and Huber loss, whereas the correlation coefficients are more or less on par for the two model types. The best performance is observed with the datasets that are subjected to data augmentation with subsequent EMSC treatment. However, the test set for the extrapolation datasets is not the same as for the other datasets, and the results should not be compared directly. EMSC in all cases improve model performance for the neural networks when comparing the pairs: Standard - EMSC, Ext. - Ext. EMSC, DA.-DA. EMSC and Ext. DA-Ext.DA EMSC, whereas the same does not seem to be the case for the PLS models. Using data augmentation seem to improve the neural network models with respect to the Huber loss, but not necessarily the RMSE. The largest improvement when using data augmentation is seen with the extrapolation datasets. Data augmentation seem to deteriorate PLS model performance unless it is combined with EMSC treatment. Figure 5 shows a side-by-side scatter plot comparison of the true and predicted reference values using the PLS and Neural network model on the Extrapolation dataset with data augmentation and subsequent EMSC treatment. There is not much difference in the training and validation sets, whereas the predictions are much closer to the ideal line for the neural network models predictions. The scatter plots show clusters, which probably corresponds to the different batches of tablets that was produced when creating the original dataset.[11]

## Discussion

The two different models were not treated consistently when tuning the two different model types. The PLS models were given an advantage by giving the tuning loop access to information about the external test set. This is not good modelling practice as it leads to overestimation of the real performance. However, this was done to counteract our biased attention to the neural network modelling. The PLS models thus represents theoretical optimal models attainable with the choice of preprocessing, where it is assumed that the perfect number of components could be found. More rigorous tuning keeping the test subset completely out of the tuning loop with either fixed validation sets or using 10 fold cross validation gave other numbers of expected optimal components and worse results. The CNN models performed better in the benchmark even though they were automatically tuned without any access to the external test set from instrument two.

It is of course possible that the performance of the PLS models could be further improved by an optimal choice of preprocessing steps, but this endeavor is best left to a method unbiased third party evaluator.

The results showed that data augmentation improve performance when training neural networks, which was expected as this has been shown in other domains[9, 8]. It was, however, a surprise that the combination of data augmentation and EMSC in combination was the best preprocessing method as the methods in theory should counteract each other. The data augmentation tries to simulate various scattering and offsets in the spectrum, whereas the EMSC tries to remove these effects. Figure 6 shows an example data augmentation of a single spectrum side-by-side with subsequent EMSC treatment. The left hand side clearly shows the variation created by the data augmentation, which the EMSC treatment then removes on the right-hand side, where the corrected spectrums lie on top of each other. However, the correction is not perfect, as visible on the zoomed inset. Residual variations are left from data augmentation even after EMSC treatment. These residuals may help the neural network focus its attention on the features that are invariant to these small shortcomings of the EMSC procedure, while at the same time benefit from the overall baseline correction from the EMSC procedure.

The extrapolation test set showed good results in the benchmark, but only if the hyperparameters were optimized with an extrapolation validation set and not randomly selected validation set. Using random selection for the validation set or cross validation gave worse results in the benchmark (results not shown). It thus seems like the network hyperparameters need to be optimized to perform well in a task that as close as possible mimics the wanted future performance. The extrapolation set was originally created to test if the networks had modelled the spectra as memberships to batches, rather than finding the inherent concentration difference between the batches, which are visible as clusters in the plots (c.f. Figure 5). The CNN models could extrapolate, which may be due to the choice of linear and semi-linear activation functions when creating the CNN models. Extrapolation is otherwise a feature missing from many non-linear models and in this respect, the choice of activation functions may be crucial.

**Kernel activations as Spectral features** To get a better understanding of the convolutional kernels, the activation of the kernels were plotted together with the average spectrum used to create the activations. Examples of the five most active kernels in convolutional layer one and two are shown in Figure 7 and 8, respectively. The plots show that the four most activated kernels in layer one has a high activation for areas of the spectrum with high values, whereas the lower valued areas are completely ignored. This

**Table 5:** Model performance on train and test set for partial least squares (PLS) and neural network models (NN). Train set includes the validation set used for tuning of hyperparameters and consists of spectrum obtained with instrument one. Test set consists of tablet samples that was never included in train and validation sets and consists of spectrums obtained with instrument two. The best performance on each test set is marked in bold.

Dataset	Subset	PLS			NN		
		R <sup>2</sup>	RMSE	Huber	R <sup>2</sup>	RMSE	Huber
Standard	Train	0.97	2.97	1.65	0.97	3.02	1.72
	Test	0.94	4.43	2.60	<b>0.97</b>	<b>4.01</b>	<b>2.51</b>
EMSC	Train	0.97	2.88	1.62	0.98	2.37	1.21
	Test	0.96	4.15	2.71	<b>0.97</b>	<b>3.17</b>	<b>1.91</b>
Ext.	Train	0.98	2.10	1.01	0.98	2.47	1.30
	Test	<b>0.36</b>	8.03	6.29	0.35	<b>4.59</b>	<b>3.22</b>
Ext. EMSC	Train	0.98	2.15	1.04	0.97	2.66	1.41
	Test	0.18	<b>3.42</b>	2.26	<b>0.33</b>	<b>3.42</b>	<b>2.09</b>
DA	Train	0.97	3.20	1.82	0.98	2.21	1.10
	Test	0.95	4.23	2.61	<b>0.97</b>	<b>3.97</b>	<b>2.44</b>
DA EMSC	Train	0.97	2.90	1.64	0.98	2.51	1.30
	Test	0.96	3.97	2.52	<b>0.98</b>	<b>3.28</b>	<b>1.89</b>
Ext. DA	Train	0.98	2.15	1.05	0.98	2.33	1.17
	Test	<b>0.38</b>	8.84	6.99	0.20	<b>3.10</b>	<b>1.79</b>
Ext. DA EMSC	Train	0.98	2.13	1.03	0.98	2.31	1.16
	Test	0.15	3.27	2.06	<b>0.52</b>	<b>1.80</b>	<b>0.88</b>

**Figure 5:** Scatter plot of true and predicted reference values using the extrapolation dataset with data augmentation followed by extended multiplicative scatter correction (EMSC). The training of the CNN model included the validation set used in the tuning of the hyperparameters. The small insert on each graph shows a zoom of the external test set.

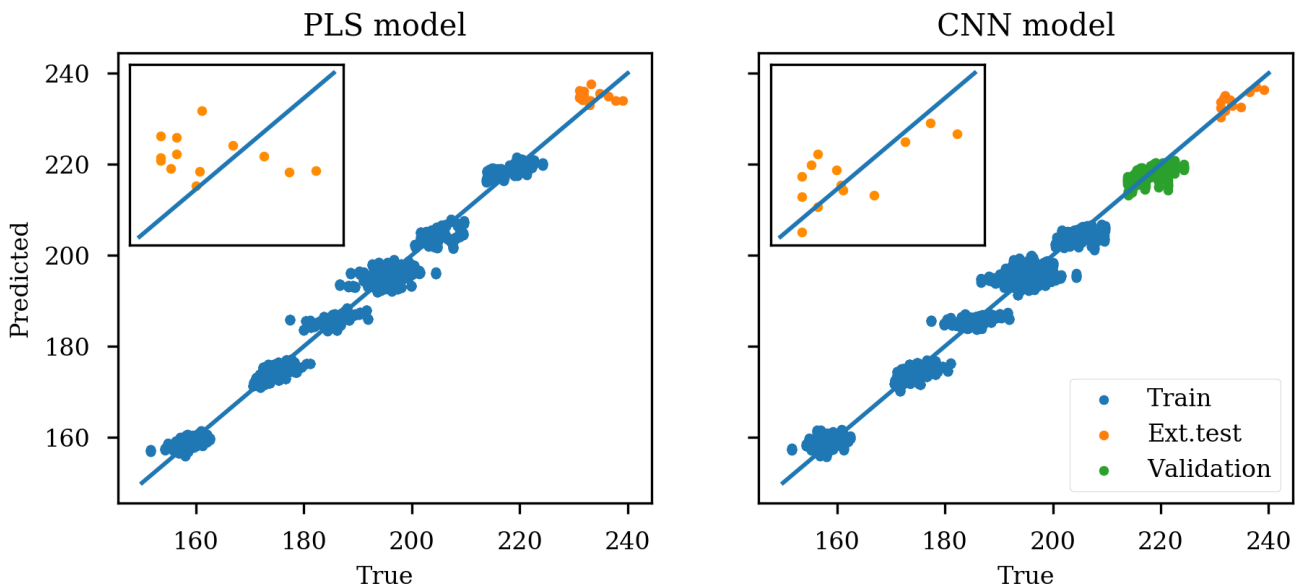


**Figure 6:** Example plot of data augmentation and data augmentation with extended multiplicative scatter correction (EMSC) of a single spectrum. A: The original spectrum is shown as solid blue line with the data augmented spectrums as dashed lines. B: The EMSC treatment employed nearly removes the data augmentation, but not completely as shown on the zoomed inset.

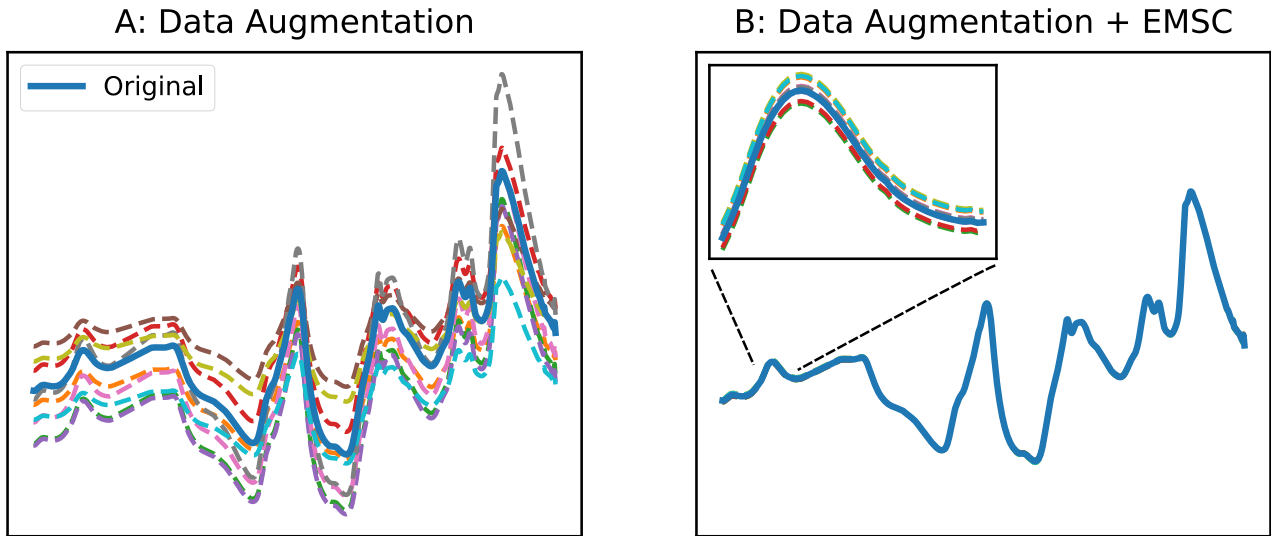


**Figure 7:** The five most active kernels for convolutional layer 1 for an example spectrum from the EMSC dataset (orange lines). The activation is shown as green lines and as the blue shading in the background.

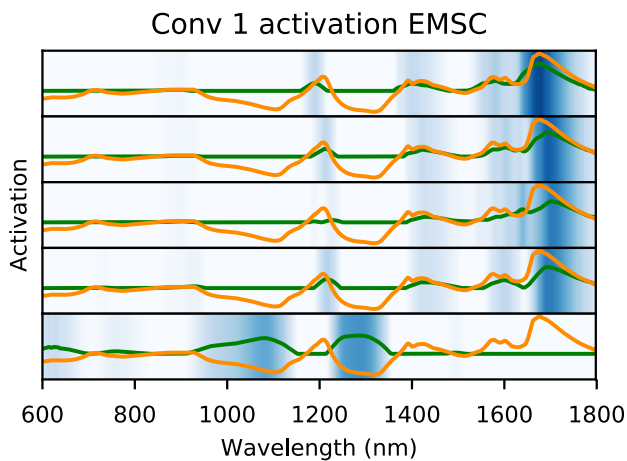
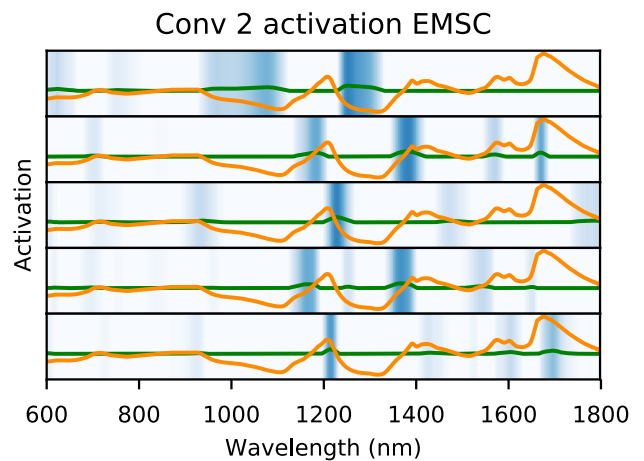


**Figure 8:** The five most active kernels for convolutional layer 2 for an example spectrum from the EMSC dataset (orange lines). The activation is shown as green lines and as the blue shading in the background.



reflects the rectified linear unit activation function, that is zero below a given threshold but otherwise linear. However, the activation of the kernels also seem dependent on the slope of the spectrum rather than the absolute value, the top points of the green lines (the activation) are offset from the top points of the orange lines (the spectrum) and the four first kernels differ slightly in this respect. The kernels thus seem to combine derivative, smoothing and threshold in varying degrees. Smoothing and using derivatives are wellknown signal processing methods as example from the wellknown Savitsky-Golay filtering and derivatisation.[27] The fifth kernel example from the convolutional layer one are instead exclusively activated at low values of the spectrum and thus more or less orthogonal to the first ones. Using orthogo-

nal features or components are the hallmark of PLS and PCA modelling. The first convolutional layer thus seems to do wellknown signal processing at least seen from a qualitative assessment. The next convolutional layer has more complex features (Figure 8). They use convolutions from the previous activations in both the spectral dimension but also the kernel dimension, and can thus make non-linear combination of these first abstractions into more complex features. The activations seen are much more specific and narrow. There is an incomplete redundancy between the kernels. The kernel example 2 and 4 seem similar with respect to the two most activated areas, but have differences in other areas. This is expected as the dropout after this layer in the neural network encourages the network to develop redundancy during training, as the redundant

---

kernels can then substitute for each other, should their activation for the next layer be dropped during training. The kernels still seem to be activated depending on the slope of the spectrum, but also dependent on the actual position on the spectrum. Some areas of the spectrum which seemingly have the same slope as activated areas are not activated at all for some of the kernels. This indicates that the kernels are working somehow like variable selection, as they are also dependent on the precise surroundings as seen in the spectrum. Variable and spectral region selection is also wellknown in spectroscopic analysis. This qualitative assessment of the kernels give an understanding about how the network can optimize itself to the task at hand and efficiently reinvent or mimic wellknown chemometric preprocessing and methods. The networks are thus not completely black box predictions as the processes up through the layers can at least be qualitatively understood and recognized, even though the precise combinations of smoothing, derivatisation and selection may be difficult to precisely decipher.

While working with the models they were found to be extremely hard to overfit, which was surprising taken the large numbers of weights in them (several million). The convolutional layers in the beginning on the other hand, have a very low number of weights and must work on all the segments from the spectrum. These first layers thus seem to work efficiently as regularization and noise reducers for the later layers which have the majority of the connections and weights, and thus efficiently reduce the problem of overfitting to noise in the data.

CNN models thus display a range of features that make them well suited for spectroscopic analysis. They can eliminate some of the need for preprocessing by mimicking known preprocessing steps such as smoothing, derivatisation and region selection, they can extrapolate in assay values and across instruments. They seem robust to overfitting due to the regularization effects of the convolutional layers. Using convolutional architectures for spectroscopy is thus likely to completely substitute the dense neural network architectures which have otherwise been employed in spectroscopy.

## Conclusion

Convolutional neural networks were used to model compound concentration in tablets, with dropout as a regularization technique. The networks could produce good results without preprocessing, but data augmentation and EMSC preprocessing were both beneficial. The counterintuitive combination of data augmentation simulating offsets in slope and intensity and subsequent removal of the offsets with EMSC worked the best, as there were residuals of the data augmentation even after EMSC correction. The neural networks showed little tendency to overfitting and in

nearly all tests surpassed standard PLS models, which was otherwise hypothetical optimal with respect to the chosen number of components. Qualitative assessment of the trained kernel activations showed that they can work as smoothing, derivative/slope recognisers, threshold and spectral region selections. The CNN models were also shown to be excellent in a hard extrapolation test, where they predicted samples from higher assay values than available in the training set and across spectrums recorded on different instruments.

## Conflict of interests

E. J. Bjerrum is the owner of Wildcard Pharmaceutical Consulting. The company is usually contracted by biotechnology/pharmaceutical companies to provide third party services.

## References

- [1] J. R. Long, V. G. Gregoriou, P. J. Gemperline, Spectroscopic calibration and quantitation using artificial neural networks, *Analytical Chemistry* 62 (17) (1990) 1791–1797.
- [2] A. Krizhevsky, I. Sutskever, G. E. Hinton, Imagenet classification with deep convolutional neural networks, in: *Advances in neural information processing systems*, 2012, pp. 1097–1105.
- [3] Y. LeCun, Y. Bengio, et al., Convolutional networks for images, speech, and time series, *The handbook of brain theory and neural networks* 3361 (10) (1995) 1995.
- [4] K. He, X. Zhang, S. Ren, J. Sun, Delving deep into rectifiers: Surpassing human-level performance on imagenet classification, in: *Proceedings of the IEEE international conference on computer vision*, 2015, pp. 1026–1034.
- [5] J. Liu, M. Osadchy, L. Ashton, M. Foster, C. J. Solomon, S. J. Gibson, Deep convolutional neural networks for raman spectrum recognition: A unified solution, *arXiv preprint arXiv:1708.09022*.
- [6] K.-J. Baik, J. H. Lee, Y. Kim, B.-J. Jang, Pharmaceutical tablet classification using a portable spectrometer with combinations of visible and near-infrared spectra, in: *Ubiquitous and Future Networks (ICUFN), 2017 Ninth International Conference on, IEEE, 2017*, pp. 1011–1014.
- [7] J. Acquarelli, T. van Laarhoven, J. Gerretzen, T. N. Tran, L. M. C. Buydens, E. Marchiori, Convolutional neural networks for vibrational spectroscopic data analysis., *Analytica chimica acta*



- 954 (2017) 22–31. doi:10.1016/j.aca.2016.12.010.
- [8] J. Wang, L. Perez, The effectiveness of data augmentation in image classification using deep learning.
- [9] E. J. Bjerrum, Smiles enumeration as data augmentation for neural network modeling of molecules, arXiv preprint arXiv:1703.07076.
- [10] N. Srivastava, G. E. Hinton, A. Krizhevsky, I. Sutskever, R. Salakhutdinov, Dropout: a simple way to prevent neural networks from overfitting., *Journal of Machine Learning Research* 15 (1) (2014) 1929–1958.
- [11] F. McClure, Designing the best possible calibration transfer procedure, [https://web.archive.org/web/20031204005143/http://www.idrc-chambersburg.org:80/shootout\\_2002.htm](https://web.archive.org/web/20031204005143/http://www.idrc-chambersburg.org:80/shootout_2002.htm) (Sep. 2017).
- [12] Nir spectra of pharmaceutical tablets from "shootout", <http://www.eigenvector.com/data/tablets/index.html> (Sep 2017).
- [13] E. Jones, T. Oliphant, P. Peterson, et al., SciPy: Open source scientific tools for Python, [Online; accessed <today>] (2001–). URL <http://www.scipy.org/>
- [14] P. Geladi, B. R. Kowalski, Partial least-squares regression: a tutorial, *Analytica chimica acta* 185 (1986) 1–17.
- [15] F. Pedregosa, G. Varoquaux, A. Gramfort, V. Michel, B. Thirion, O. Grisel, M. Blondel, P. Prettenhofer, R. Weiss, V. Dubourg, et al., Scikit-learn: Machine learning in python, *Journal of Machine Learning Research* 12 (Oct) (2011) 2825–2830.
- [16] P. J. Huber, et al., Robust estimation of a location parameter, *The Annals of Mathematical Statistics* 35 (1) (1964) 73–101.
- [17] H. Martens, E. Stark, Extended multiplicative signal correction and spectral interference subtraction: new preprocessing methods for near infrared spectroscopy., *Journal of pharmaceutical and biomedical analysis* 9 (1991) 625–635.
- [18] R. M. Jarvis, D. Broadhurst, H. Johnson, N. M. O'Boyle, R. Goodacre, Pychem: a multivariate analysis package for python., *Bioinformatics (Oxford, England)* 22 (2006) 2565–2566. doi:10.1093/bioinformatics/bt1416.
- [19] F. Chollet, keras, <https://github.com/fchollet/keras> (2015).
- [20] R. Al-Rfou, G. Alain, A. Almahairi, C. Angermueller, D. Bahdanau, N. Ballas, F. Bastien, J. Bayer, A. Belikov, A. Belopolsky, Y. Bengio, A. Bergeron, J. Bergstra, V. Bisson, J. Blecher Snyder, N. Bouchard, N. Boulanger-Lewandowski, X. Bouthillier, A. de Brébisson, O. Breuleux, P.-L. Carrier, K. Cho, J. Chorowski, P. Christiano, T. Cooijmans, M.-A. Côté, M. Côté, A. Courville, Y. N. Dauphin, O. Delalleau, J. Demouth, G. Desjardins, S. Dieleman, L. Dinh, M. Ducoffe, V. Dumoulin, S. Ebrahimi Kahou, D. Erhan, Z. Fan, O. Firat, M. Germain, X. Glorot, I. Goodfellow, M. Graham, C. Gulcehre, P. Hamel, I. Harlouchet, J.-P. Heng, B. Hidas, S. Honari, A. Jain, S. Jean, K. Jia, M. Korobov, V. Kulkarni, A. Lamb, P. Lambin, E. Larsen, C. Laurent, S. Lee, S. Lefrançois, S. Lemieux, N. Léonard, Z. Lin, J. A. Livezey, C. Lorenz, J. Lowin, Q. Ma, P.-A. Manzagol, O. Mastropietro, R. T. McGibbon, R. Memisevic, B. van Merriënboer, V. Michalski, M. Mirza, A. Orlandi, C. Pal, R. Pascanu, M. Pezeshki, C. Raffel, D. Renshaw, M. Rocklin, A. Romero, M. Roth, P. Sadowski, J. Salvatier, F. Savard, J. Schlüter, J. Schulman, G. Schwartz, I. V. Serban, D. Serdyuk, S. Shabanian, E. Simon, S. Spieckermann, S. R. Subramanyam, J. Sygnowski, J. Tanguay, G. van Tuler, J. Turian, S. Urban, P. Vincent, F. Visin, H. de Vries, D. Warde-Farley, D. J. Webb, M. Willson, K. Xu, L. Xue, L. Yao, S. Zhang, Y. Zhang, Theano: A Python framework for fast computation of mathematical expressions, arXiv e-prints abs/1605.02688. URL <http://arxiv.org/abs/1605.02688>
- [21] J. Nickolls, I. Buck, M. Garland, K. Skadron, Scalable parallel programming with cuda, *Queue* 6 (2) (2008) 40–53.
- [22] M. D. Zeiler, D. Krishnan, G. W. Taylor, R. Fergus, Deconvolutional networks, in: *Computer Vision and Pattern Recognition (CVPR), 2010 IEEE Conference on*, IEEE, 2010, pp. 2528–2535.
- [23] V. Dumoulin, F. Visin, A guide to convolution arithmetic for deep learning, arXiv preprint arXiv:1603.07285.
- [24] V. Nair, G. E. Hinton, Rectified linear units improve restricted boltzmann machines, in: *Proceedings of the 27th international conference on machine learning (ICML-10)*, 2010, pp. 807–814.
- [25] M. D. Zeiler, Adadelta: an adaptive learning rate method, arXiv preprint arXiv:1212.5701.
- [26] T. G. authors, Gpyopt: A bayesian optimization framework in python,

---

<http://github.com/SheffieldML/GPyOpt>  
(2016).

- [27] A. Savitzky, M. J. Golay, Smoothing and differentiation of data by simplified least squares procedures., *Analytical chemistry* 36 (8) (1964) 1627–1639.